ELSEVIER

Polymer 43 (2002) 6247–6254

polymer

www.elsevier.com/locate/polymer

Observation of a fast dielectric relaxation in semi-crystalline poly(ethylene oxide)

Xing Jin, Shihai Zhang, James Runt*

Department of Materials Science Engineering and Materials Research Institute, Pennsylvania State University, University Park, PA 16802, USA

Received 20 May 2002; received in revised form 7 August 2002; accepted 9 August 2002

Abstract

Our broadband dielectric study has revealed for the first time a relaxation (termed γ') between the low temperature β and γ-processes of semi-crystalline poly(ethylene oxide) (PEO). The activation energy of the γ'-transition is indicative of a local process, and this relaxation becomes broader with increasing temperature. We propose that this process is due to the motion of PEO segments in the transition region between PEO lamellae and disordered interlamellar amorphous segments. The unusual local character of the γ'-process is explained by analogy to the fast process or primitive α-relaxation in nanoconfined glass forming systems. This mechanism is supported by comparison of the dielectric behavior of samples with different thermal histories.

Keywords: Poly(ethylene oxide); Relaxation behavior; Dielectric

1. Introduction

Over the last several decades there have been extensive reports of the relaxation behavior of semi-crystalline polymers [1–3] and poly(ethylene oxide) (PEO) has sometimes been used as a model, highly crystalline material in such studies. In addition, PEO has attracted interest as a consequence of its potential in high-energy density devices. In early measurements of mechanical and dielectric loss [4–7], PEO was found to exhibit three major relaxations below its melting point (T_m). These are generally referred to as the α, β and γ-processes, with decreasing temperature [8]. The α-relaxation is a local process associated with the crystalline phase. It generally cannot be observed in dielectric studies due to high dc conductance at higher temperatures and lower frequencies, although some authors have attempted to separate it out [6,9]. It has been reported that the cooperative β-process is absent in the dielectric spectrum of a PEO single crystal mat (PEO molecular weight (MW) $> 10^5$), while the γ-process remains. Together with other experimental results, this indicates that the β-process originates in cooperative segmental motions only in a portion of the non-crystalline component, and that this motion is not possible in the fold surfaces of single crystals. This is presumably true for segments in the fold surfaces ('interphase') of melt-crystallized PEO as well. Early on, the lower temperature γ-process was assigned to local twisting in the main chains in both defective regions within crystallites and non-crystalline regions, including amorphous segments in the fold structure on crystal surfaces. However, more recently, the γ-process in other highly crystalline polymers has been assigned to local motions in the amorphous phase only [1].

In a relatively recent dielectric study of an immiscible blend of 5% of a low molecular weight PEO in polystyrene [10], Smith et al. reported a relaxation located between the α and β processes, which they termed β'. They proposed that this process was associated with segmental motion of amorphous chains perturbed by being tethered to crystallites. This observation is reminiscent of the two glass transition temperatures (T_g) reported in studies of PEO by differential scanning calorimetry (DSC) and thermal expansion data [11,12]. A higher temperature glass transition, referred to in earlier literature as $T_g(U)$, was proposed to arise from amorphous segments under relatively more constraint by crystallites, and the lower T_g, $T_g(L)$, from amorphous segments completely or relatively free from constraint [12].

An important feature of the solid-state structure of melt-crystallized polymers is the transition region between the crystals and isotropic disordered segments, i.e. the so-called

* Corresponding author. Tel.: +1-814-863-2749; fax: +1-814-865-2917.
E-mail address: runt@matse.psu.edu (J. Runt).

0032-3861/02/$ - see front matter
PII: S0032-3861(02)00560-8

'interphase'. These transition regions have been proposed theoretically [13,14] and observed experimentally, principally in experiments on polyethylene (PE) [15,16]. The order–disorder transition has been estimated to occur over a spatial range of 1–3 nm for linear PE. Since interlamellar regions in polymers with high degrees of crystallinity like PEO are on the order of 6–7 nm [17,18], chain segments in interphase regions comprise a rather significant portion of all non-crystalline segments.

As a preamble to our exploration of the dielectric relaxation behavior of melt-miscible blends of PEO with amorphous polymer diluents, we describe in this paper the results of a broadband dielectric study of semi-crystalline PEO. For the first time, we observe a relaxation located between the β and γ processes, which we refer to as γ′, and assign it to the relaxation of segments in the interphase region.

2. Experimental section

2.1. Materials

The PEO used in these experiments was purchased from Polysciences. M_w and M_n were determined from gel permeation chromatography (GPC) to be 2.16×10^5 and 5.36×10^4, respectively. Dimethylformamide containing 0.05 M LiBr was used as the mobile phase in the GPC experiments. Calibration was performed using nearly monodisperse ($M_w/M_n < 1.1$) PEO standards (Polymer Standards Service, USA), ranging from 10 000 to 963 000 g/mol.

PEO powder was pressed at 100 °C with slight pressure in a Carver hydraulic press for an hour. The molecular weight was determined by GPC after pressing and found to be essentially the same as that before heating. Samples were cooled from the melt using different procedures. Sample A was taken from the press and directly cooled in air to room temperature. Sample B was immediately transferred into an oven and crystallized at 54 °C under vacuum for 24 h. The samples were stored in a desiccator at room temperature prior to the dielectric experiments. Dielectric spectra were acquired for each sample 24 h after processing ('unaged'). In addition, sample A was aged in a desiccator (at room temperature) and the dielectric spectra determined after 80 days.

2.2. Differential scanning calorimetry

Degrees of crystallinity and nominal T_ms were determined using a Perkin–Elmer DSC-7. Sample weights were about 10 mg. Temperature and transition enthalpies were calibrated using an indium standard. Heats of fusion were converted to degrees of crystallinity using a perfect crystal heat of fusion for PEO of 203 J/g [19]. The heating rate used in all experiments was 10 °C/min.

2.3. Dielectric experiments

Dielectric relaxation spectra were collected using a Novocontrol Concept 40 broadband dielectric spectrometer. Temperature control was accomplished with a Novocontrol Quatro Cryosystem. Experiments were run in the frequency domain (0.01 Hz–10 MHz) and between −140 and 25 °C in 2.5, 5 or 7.5 °C increments. Temperature stability was ±0.1 °C, and the minimum stabilization time set at any given temperature was 1 min. Samples were cooled and heated in the presence of N_2 during the dielectric measurements. Dielectric specimens were 0.2–0.5 mm thick, and were coated with a thin layer of gold on both sides to optimize electrical contact, then sandwiched between two electrodes having a diameter of 20 mm.

2.3.1. Dielectric data processing

Isothermal dielectric loss curves were fit with one or more Havriliak–Negami (HN) functions and a dc loss contribution (if necessary). The general expression used in the fitting (including a dc loss contribution) can be written as [20]

$$\varepsilon(\omega) = \varepsilon' - \mathrm{i}\varepsilon'' = \sum\left[\frac{\varepsilon_\infty - \varepsilon_0}{(1+(\mathrm{i}\omega\tau)^a)^b} + \varepsilon_\infty\right] - \mathrm{i}\left[\frac{\sigma}{\varepsilon_v \omega}\right]^N \quad (1)$$

where the summation symbol is used in our case since more than one relaxation process can exist in the frequency range of the curve fitting. The symbols ε_∞ and ε_0 are the limiting dielectric constants at infinitely high and low frequencies, respectively; ω, the angular frequency; τ, the characteristic relaxation time of the process; σ, the conductivity; ε_v, the vacuum permittivity, 8.85×10^{-12} F/m and N is an exponent that characterizes the conduction process. N was fixed at 0.65 after simulation with different values. The exponents a and b ($0 < a, b < 1$) are shape parameters: a is an indicator of the breadth of the relaxation, and $a = \partial\log\varepsilon''/\partial\log f$ at $f \ll f_0$, a characteristic frequency related to τ. The parameter b represents the asymmetry of the curve and $ab = -\partial\log\varepsilon''/\partial\log f$ at $f \gg f_0$. The dielectric relaxation strength, $\varepsilon_\infty - \varepsilon_0$, will be represented as $\Delta\varepsilon$.

At most experimental temperatures, more than one relaxation process was present in the measurement frequency range and were not well separated, making curve fitting challenging. To facilitate analysis, loss data were plotted vs. temperature and the temperatures of maximum loss (T_{max}) determined. The frequency of maximum loss (f_{max}) at different experimental temperatures was then back calculated from an Arrhenius plot and used as the initial value of τ in the curve fitting. Attention was paid to the results of the fitting to ensure that all parameters change continuously with temperature and that the experimental dielectric constant (ε')—frequency data were also adequately fit using the same parameters as determined from the loss data. The first frequency spectrum to be analyzed

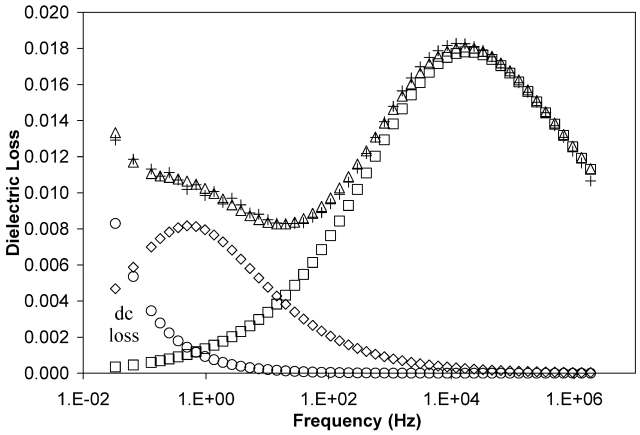

Fig. 1. The comparison of the HN fitting results with the experimental data at −87.5 °C for unaged sample A. (+) Experimental data; triangles: fitted results; circles: dc loss; diamonds: the γ′-process; squares: the γ-process.

for a given sample was at a temperature where the different relaxations were relatively well separated and a significant portion of the peak(s) of interest were evident in the experimental frequency range. The temperature dependence of the fitting parameters was determined from these fits, then data at other temperatures were fit following the established temperature dependencies. Fig. 1 provides an example of the curve fitting of the dielectric loss for unaged sample A at −87.5 °C.

3. Results and discussion

3.1. Degrees of crystallinity

Degrees of crystallinity determined by DSC for samples A and B as a function of aging time are displayed in Fig. 2. The initial value for sample A was measured within 1.5 h of its return to room temperature and within 4 h for sample B. The experimental uncertainty associated with the data points in Fig. 2 are on the order of ±2% crystallinity. The

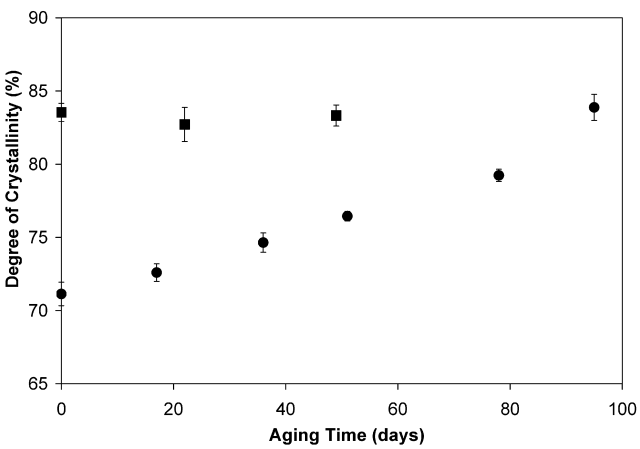

Fig. 2. Degree of crystallinity as a function of aging time. Filled circles: sample A; filled squares: sample B.

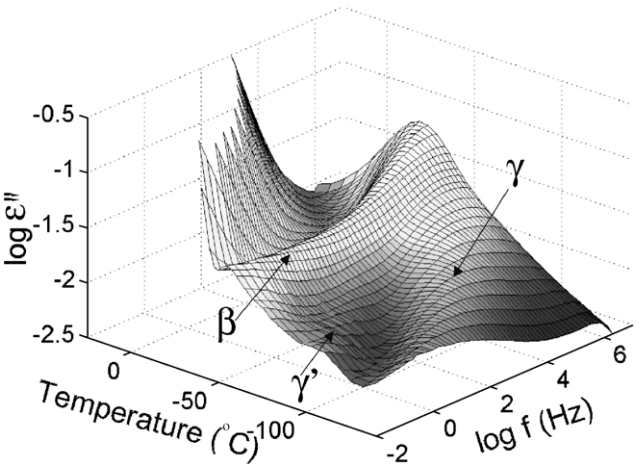

Fig. 3. 3D dielectric loss spectra of unaged sample A.

initial crystallinity of sample A is 70%, while that of isothermally crystallized B is considerably higher (83%), and the latter remains unchanged during storage. Sample A's crystallinity continues to increase slowly on aging at room temperature, reaching the level of sample B after aging for ~100 days. The nominal melting point of A also increases by about 2 °C during aging, but is still ~3 °C below the T_m of sample B after ~100 days.[1] The implication is that some lamellar thickening occurs during the aging of sample A (at a temperature corresponding to a degree of supercooling (ΔT) of ~45 °C, and ~80 °C above the PEO T_g).

3.2. Dielectric relaxation

Fig. 3 displays the 3D dielectric loss spectra for unaged specimen A. The location of the various relaxations can be seen more readily in Fig. 4. Three distinct relaxation processes are apparent: the β and γ processes appear at relatively high and low temperatures, respectively. The dc conductance, which dominates at relatively low frequency and high temperature, decreases from ~10^{-12} to 10^{-16} S/cm as temperature is reduced from −10 to −40 °C (i.e. above T_g) and the apparent activation energy (E_a) for the conduction was determined to be ~62 kJ/mol. Aged samples A and B have similar relaxation behavior as unaged sample A.

A third process, not reported previously, is located between the β and γ processes and is denoted here as γ′. The activation energies calculated from the slope of the Arrhenius plots in Fig. 4 are 193, 15 and 21 kJ/mol for the β, γ, γ′ processes, respectively. The reason why the γ′-relaxation has not been observed in previous dielectric studies of PEO is likely related to the relatively broad

[1] Melting points are not presented, in order to deemphasize specific values. Since relatively large sample sizes were used in the experiments, apparent peak melting points are artificially raised due to thermal lag during the DSC experiments, resulting from low polymer thermal conductivity.

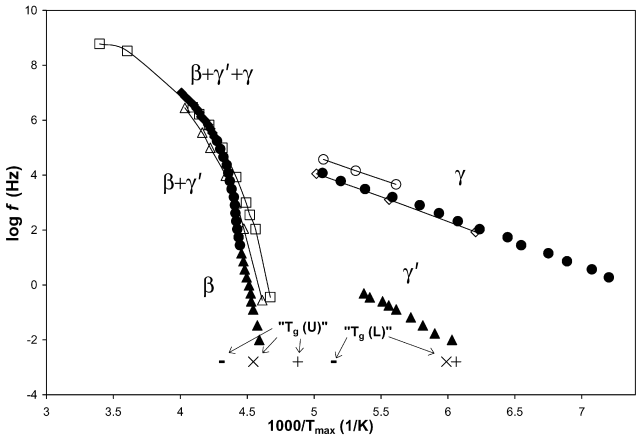

Fig. 4. Arrhenius plot for unaged sample A, compared with published data. Filled symbols: unaged sample A; unfilled symbols: data from literature. Data from Ref. [7] (squares: MW = 2.8×10^6; triangles: MW = 8.4×10^5; circles: single crystals; diamonds: melt-crystallized). Data from Ref. [11] (slash: reported; (×) onset points); (+) data from Ref. [12].

experimental frequency window available in our experiments. The β-relaxation merges with the γ′ and γ processes as frequency increases, and the merged processes are labeled as β + γ′ and β + γ′ + γ, having E_a of 188 and 54 kJ/mol, respectively. The frequency–temperature locations of the β, γ and merged relaxations agree very well with those collected and published previously (Fig. 4) [8].

From the 3D dielectric loss spectra, and with the aid of the Arrhenius plot, it can be seen that in the 2D spectra of dielectric loss vs. frequency, the γ′ and γ relaxations are the low and high frequency peaks, respectively, below T_g. The β-process is far beyond the low frequency portion of the spectra until close to T_g, when it moves rapidly into the experimental frequency range. The β-process then merges with the γ′-relaxation when temperature is further increased by only ∼5 °C, which in turn merges with the γ-process after an additional ∼15 °C. Note that in early studies the β-process was incorrectly believed to be the dominant process at all temperatures [4,8]. This can easily lead to unreasonable conclusions concerning the β-relaxation from 2D dielectric loss spectra.

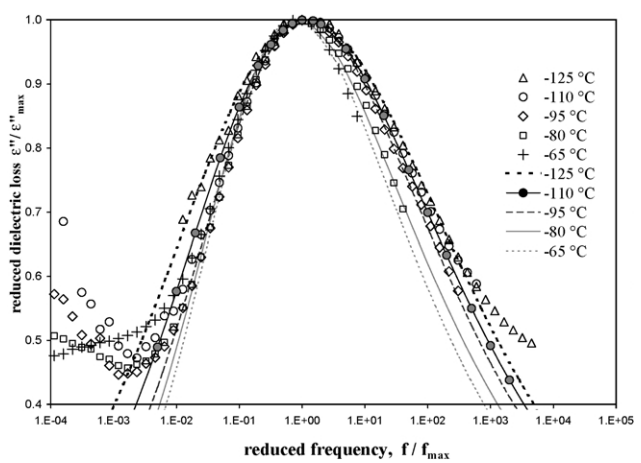

Fig. 5. The normalized dielectric spectra of the γ-relaxation of unaged sample A at selected temperatures. The solid and dashed lines represent the HN fits to the relaxations.

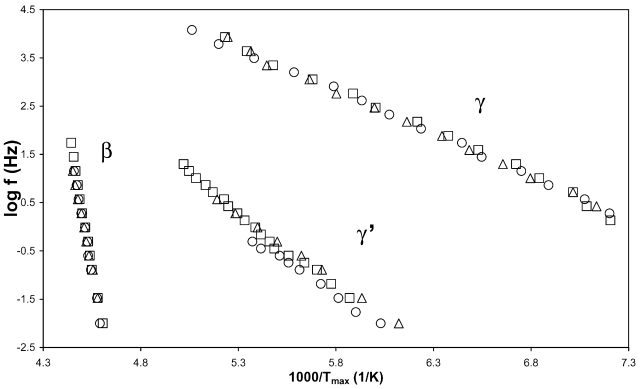

Fig. 6. Relaxation map of the β, γ′ and γ processes for aged and unaged samples A and B. Circles: unaged sample A; triangles: aged sample A; squares: sample B.

The broad γ-relaxation dominates the loss spectra at most experimental temperatures and normalized loss plots were created to evaluate the shape of the γ-process at different temperatures. At the temperatures selected in Fig. 5, the γ′-process (at lower frequency) does not appreciably overlap with the γ-relaxation. The γ-process becomes narrower with increasing temperature, due to a narrowing in the distribution of local environments. The shape of the PEO γ-process in amorphous blends of PEO with other miscible polymers is nearly identical to that associated with neat crystalline PEO [21], in general agreement with the assignment of the γ-process to non-crystalline segments [1].

Fig. 6 shows the relaxation map of the β, γ′ and γ relaxations of the three different samples investigated in this study. The data points for the β and γ processes of all samples overlap considerably, while those for the γ′-relaxation are very similar but vary a bit more among the different samples. The HN fit parameters for all relaxations of unaged sample A are shown in Fig. 7. Those for aged A and isothermally crystallized B, as a function of temperature,

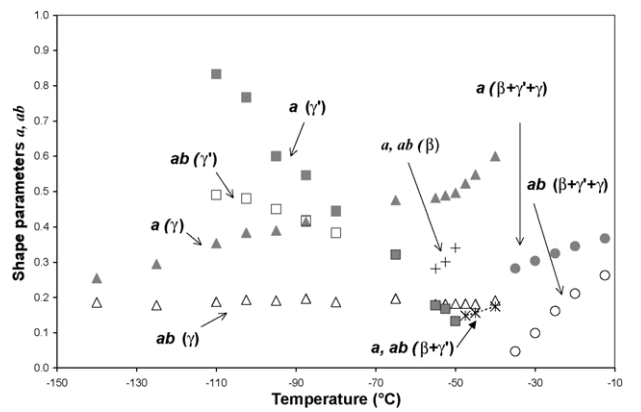

Fig. 7. HN shape parameters of the dielectric relaxations of unaged sample A. Filled symbols: parameter *a*; hollow symbols: parameter *ab*.

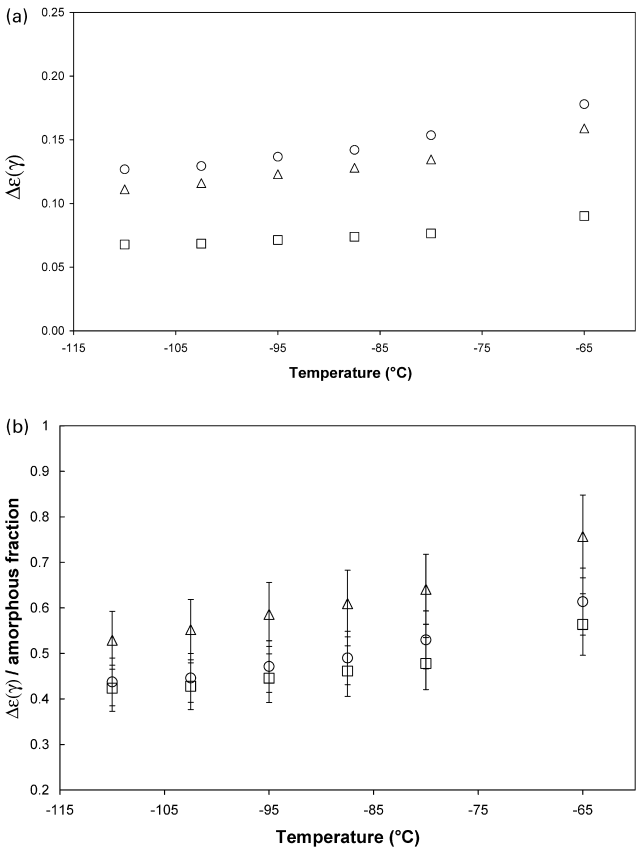

Fig. 8. (a) Relaxation strengths of the γ-process of all three samples as a function of temperature. Circles: unaged sample A; triangles: aged sample A; squares: sample B. (b) Relaxation strengths normalized to the amorphous fraction in each of the samples, as a function of temperature.

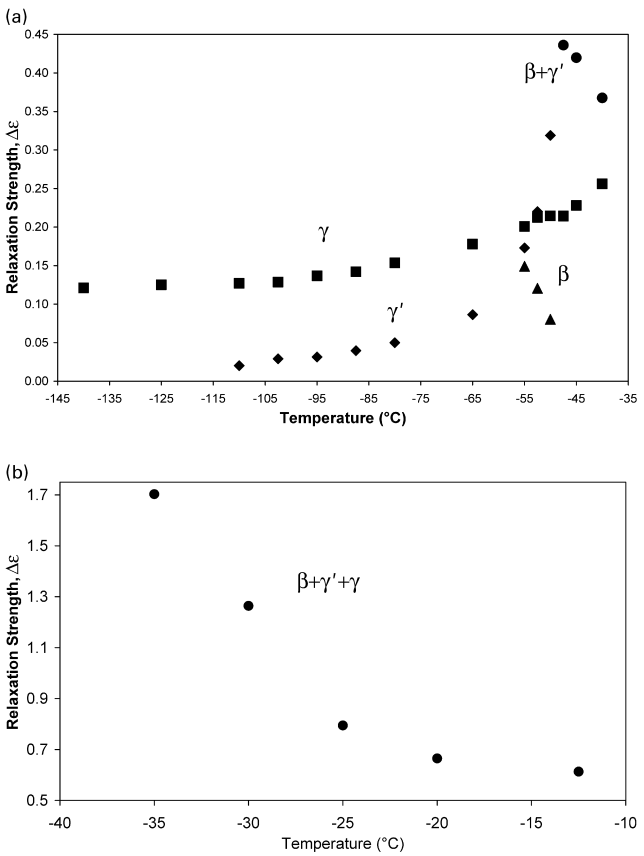

Fig. 9. Relaxation strengths of all processes of unaged sample A.

are very similar. With increasing temperature the γ′-relaxation in all samples becomes more symmetric ($a \rightarrow ab, b \rightarrow 1$). In addition, the frequency distribution of the γ′-relaxation (as indicated by the fit parameters in Fig. 7) becomes *broader* with increasing temperature for all three samples, opposite to the behavior of the β and γ processes.

3.2.1. Relaxation strengths

The relaxation strengths of the local γ-process at selected temperatures for all three samples are presented in Fig. 8(a). $\Delta\varepsilon(\gamma)$ for the higher crystallinity aged sample A and, particularly, sample B are lower than that of unaged sample A, in general agreement with at least partial amorphous origin of the γ-process. If the γ-relaxation is of completely amorphous origin, the ratio of $\Delta\varepsilon(\gamma)$ to the fraction of non-crystalline segments in each sample should be constant. Fig. 8(b) presents this normalized relaxation strength for the three samples at selected temperatures. The relative uncertainty in dielectric strength is about 10%. Together with the uncertainty in the crystallinity measurement this leads to a calculated total uncertainty of $\sim \pm 12\%$. Clearly, the ratios of the three samples cannot be distinguished within experimental error.

The relaxation strengths of the various individual and merged processes are shown in Fig. 9 for unaged specimen A. $\Delta\varepsilon$ for the β, merged $\beta + \gamma' + \gamma$ and $\beta + \gamma'$ processes decrease with increasing temperature, while those of the γ′ and γ relaxations increase. Based on generalizations formed mainly from amorphous systems, the former behavior is believed to be characteristic of cooperative processes and the latter with local relaxations.

3.3. Origin of the γ′-relaxation

What is the origin of the γ′-process? In any multiphase system one must first consider the possibility of a Maxwell–Wagner–Sillars (MWS) mechanism. However, neither phase has appreciable conductivity (σ) in the temperature range of the γ′-relaxation (i.e. $\sigma_c - \sigma_a$ is very small). An estimate [22] of the relaxation time of an MWS process leads to predicted frequencies $\leq 10^{-5}$ Hz, ruling out an interfacial polarization mechanism as the origin of the γ′-process.

The second possibility considered was that the γ′-process is due to absorbed moisture. Several PEO samples were placed into a sealed bottle, and suspended over a pool of water. Dielectric spectra at −95 °C for samples exposed to water vapor for different time periods are compared in Fig. 10. The γ′ and γ processes move to higher and lower frequencies, respectively, with increasing moisture content, and merge at the longest hydration time. Increasing water

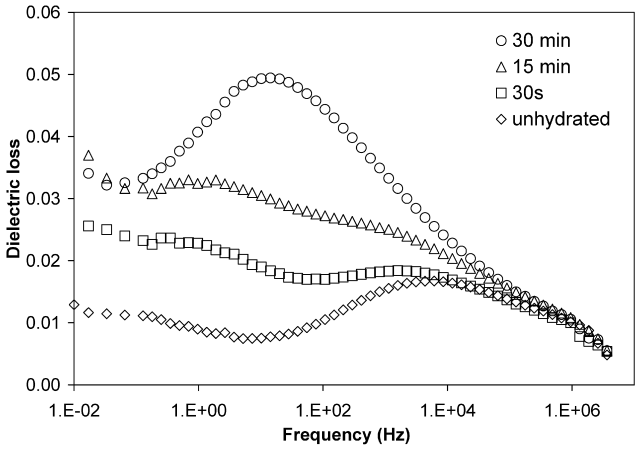

Fig. 10. Dielectric spectra of PEO at −95 °C at selected hydration times.

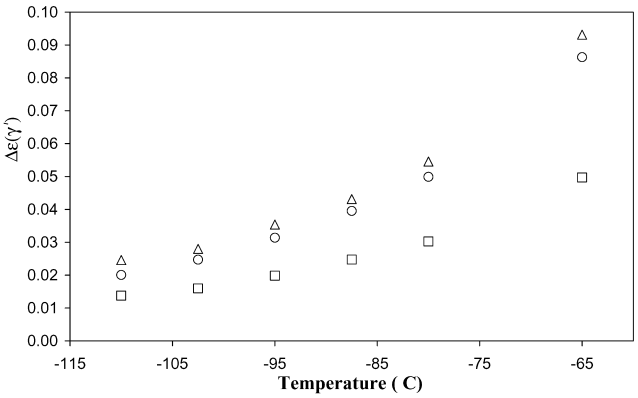

Fig. 11. The relaxation strength of the γ′-process as a function of temperature for the three PEO samples. Circles: unaged sample A; triangles: aged sample A; squares: sample B.

content is also accompanied by increasing dc conduction. If the γ′-process is associated strictly with water, its frequency location would not be expected change, and its strength should clearly increase, with increasing water content. However, neither of these is the case.

Additional aging experiments were conducted on PEO specimens, crystallized in a different fashion than samples A and B. The relaxation strength of the γ′-process was observed to decrease on aging, inconsistent with a relaxation due to absorbed moisture. Given the evidence at hand, we conclude that the γ′-process is not associated with moisture, and it must therefore originate from PEO itself.

Based on the evidence presented below, it is proposed that the γ′-relaxation involves segments in the order–disorder transition region. The interphase region is envisioned as consisting of tight chain folds that reenter the lamella at a neighboring position and are unable to relax cooperatively; looser folds; a portion of cilia protruding from lamellae; and a portion of tie molecules connecting neighboring lamellae. This transition zone has been estimated to be ~2 nm thick for PEO [17,23] and segments in such regions consequently make up a significant portion of the total number of amorphous units, considering that the total interlamellar width is only 6–7 nm. Consequently, it is not surprising that the relaxation strength of the γ′-process is similar to $\Delta\varepsilon(\beta)$ (Fig. 9). $\Delta\varepsilon(\gamma')$ of the aged and unaged versions of sample A are indistinguishable within experimental error, but are about a factor of two larger than the strength of the γ′-relaxation of sample B (Fig. 11). At equivalent crystallinity, the interphase fraction in aged sample A is expected to be larger than that of B due to thicker lamellae in the latter (resulting from a higher mean T_c) and more rapid initial crystallization of sample A.

The assignment of the γ′-relaxation to the order–disorder transition region can also explain its unusual broadening behavior. Recall that this process becomes broader with increasing temperature (see the decreasing HN shape parameters in Fig. 7), opposite to the generally observed narrowing of both cooperative and local relaxations with increasing temperature. The special behavior of the γ′-relaxation cannot be explained by assigning it to disordered interlamellar amorphous segments, but can be rationalized by invoking the interphase. When temperature increases from below T_g, the disordered amorphous component on one side of interphase region becomes more mobile, but the crystalline phase on the other remains rigid until T_m. Therefore, the environmental asymmetry of the order–disorder region becomes larger with increasing temperature, resulting in a broader frequency distribution for the γ′-relaxation.

One question remains to be answered: why is γ′ a local process? The evidence at hand leads us to propose that the γ′-relaxation is similar to the ‘fast process’ in nanoconfined glass forming systems [24–27]. It is generally believed that a pure confinement effect leads to a reduction in T_g, while strong surface interactions increase T_g [28,29]. The reduction in T_g upon confinement has been explained by invoking the cooperatively rearranging region (CRR) concept [30]. The glass transition, or equivalently the segmental relaxation, is a cooperative process and is only possible through the accompanying motion of other repeat units in a minimum volume, i.e. the CRR. If the scale of the confinement is smaller than the CRR, normal segmental relaxations will be limited and a modified process emerges, which involves fewer repeat units and sometimes becomes a non-cooperative process. This leads to a decrease in T_g and relaxation time, since a smaller relaxation unit is involved.

The above analogy to nanoconfinement is also supported by a study on PEO-layered silicate nanocomposites. PEO (MW ~ 10^5) was found to be intercalated in ~0.8 nm galleries between silicate layers, and the motion of the intercalated segments was found to be relatively non-cooperative compared with the T_g motion of amorphous segments in bulk samples [31]. The proposed assignment is further supported by a study of PEO chains ($M_w = 2 \times 10^3$ and 6×10^3) tethered on a silica surface [32], where the ‘tail’ segments (similar to the interphase in that segments

are bounded by a rigid wall) protruding from the surface were found to have greater mobility than segments in amorphous regions in bulk PEO.

The faster γ'-relaxation can also be explained by the primitive α-relaxation concept [25]. Some segments in looser folds and cilia will be oriented more or less perpendicular to the lamellar surface and separated by tight folds. One can therefore argue that these segments will experience less entanglement and reduced intermolecular constraints compared with Gaussian chains between lamellae. A non-cooperative and faster relaxation process would then be expected.

The β-relaxation remains a cooperative process since the distance between interfacial regions is comparable to or larger than the size of the CRR ($\sim$2–3 nm at T_g). Confinement experienced by disordered PEO segments in this region arises primarily from the interphases, which are relatively 'soft' (with the degree of order varying through the structure) and thus will not be as effective as a hard wall in constraining the cooperative β-relaxation.

Angell [33] has reported that the temperature at which the relaxation time for the fundamental enthalpy relaxation process reaches 100 s is close to the T_g obtained from standard calorimetric measurements—specifically, the temperature at which the heat capacity jump commences at a heating rate of 10 °C/min. The location of the two T_gs reported for PEO in Ref. [10] are plotted in Fig. 4, assuming an effective frequency of 1.6×10^{-3} Hz ($\sim$100 s), although this assumption may be somewhat less suitable for sub-T_g transitions. The calorimetric T_g values are much higher than estimates from extrapolation of our β and γ' processes data to lower frequencies. However, the two transitions shown in Ref. [11] are $\sim$10–25 °C wide, and the end point of the transition was used to define 'T_g' in Ref. [10]. Consequently, we also plot in Fig. 4 the onset temperatures of the heat capacity change. The locations of the β and γ' transitions extrapolate relatively near to the onset T_g values.

3.4. Merging of the β-relaxation with the γ' and γ processes

The merging of relaxations in glass forming systems, including polymers, is a long-standing topic [34,35]. When the cooperative size scale decreases to the size of the interphase, the interphase segments originally involved in the γ'-relaxation also begin to participate in the overall cooperative segmental relaxation. This scenario is consistent with the observation that the slope of the Arrhenius plot for the $\beta + \gamma'$ process is almost the same as that of the β-process, and the initial value of $\Delta\varepsilon(\beta + \gamma')$ is approximately the sum of the extrapolated $\Delta\varepsilon(\beta)$ and $\Delta\varepsilon(\gamma')$.

Near the temperature where the $\beta + \gamma'$ and γ processes merge, $\Delta\varepsilon(\beta + \gamma' + \gamma)$ increases stepwise to twice that of $\Delta\varepsilon(\beta + \gamma') + \Delta\varepsilon(\gamma)$. Sy and Mijovic [36] reported a similar jump of $\Delta\varepsilon$ from the local process to the merged local and cooperative segmental process, through the T_g of poly(methyl methacrylate) (PMMA) and its blends with poly(vinylidene fluoride), while Dionísio et al. [37] filled the gap around T_g of neat PMMA with gradually increasing $\Delta\varepsilon$ values. The merging of β and γ relaxations is typical of mergence of cooperative and local relaxations. The relaxation times of the two processes become comparable at the merging point. The two processes were originally separated, but are correlated and merged into a new process, the details of which require further study.

4. Summary

Our broadband dielectric study revealed three relaxations below the melting point of PEO: the β, γ', and γ relaxations, with decreasing temperature. The cooperative β-process arises from the segmental relaxation of disordered PEO amorphous segments and the γ-process from the local main chain twisting of the non-crystalline component. We attribute the dielectric γ'-relaxation to the motion of PEO segments in the transition regions between the lamellae and the disordered interlamellar amorphous segments. The unusual local character of the γ'-process is explained well by invoking nanoconfinement from the lamellae and an immobile amorphous phase below T_g. This mechanism is supported by comparison of the dielectric behavior of samples with different preparation histories.

Acknowledgements

We would like to express our appreciation to the National Science Foundation, Polymers Program (DMR—9900638 and 0211056) for its support of this research and the NSF-MRI program for support of the dielectric instrumentation (DMR-0079432). We would also like to thank Dr Evangelos Manias for helpful discussions.

References

[1] Boyd RH. Polymer 1985;26:323.
[2] Boyd RH. Polymer 1985;26:1123.
[3] Boyd RH, Liu F. In: Runt JP, Fitzgerald JJ, editors. Dielectric spectroscopy of polymer materials: fundamentals and applications. Washington, DC: American Chemical Society; 1997. p. 107.
[4] Connor TM, Read BE, Williams G. J Appl Chem 1964;14:74.
[5] Ishida Y, Matsuo M, Takayanagi M. J Polym Sci, Polym Lett 1965;3:321.
[6] Porter CH, Boyd RH. Macromolecules 1971;4:589.
[7] Enns JB, Simha R. J Macromol Sci 1977;B13(1):25.
[8] McCrum NG, Read BE, Williams G. Anelastic and dielectric effects in polymer solids. New York: Dover; 1967. p. 540.
[9] Fanggao C, Saunders GA, Lambson EF, Hampton RN, Carini G, Marco Gdi, Lanza M. J Polym Sci, Polym Phys 1996;34:425.
[10] Smith TW, Abkowitz MA, Conway GC, Luca DJ, Serpico JM, Wnek GE. Macromolecules 1996;29:5042.
[11] Lang MC, Noel C. J Polym Sci, Polym Phys 1977;15:1319.
[12] Boyer RF. J Polym Sci, Polym Symp 1975;50:189.
[13] Kumar SK, Yoon DY. Macromolecules 1991;22:5414.

[14] Gautam S, Balijepalli S, Rutledge GC. Macromolecules 2000;33: 9136.
[15] Mandelkern L, Alamo RG, Kennedy MA. Macromolecules 1990;23: 4721.
[16] Pang W, Fan C, Zhu Q. Eur Polym J 2001;37:2425.
[17] Talibuddin S, Wu L, Runt J, Lin JS. Macromolecules 1996;29:7527.
[18] Lisowski MS, Liu Q, Cho J, Runt J, Yeh F, Hsiao BS. Macromolecules 2000;33:4842.
[19] Wunderlich B, Macromolecular physics, vol. 3. New York: Academic Press; 1980.
[20] Havriliak Jr.S, Havriliak SJ. Dielectric and mechanical relaxation in materials: analysis, interpretation, and application to polymers. Cincinnati: Hanser; 1997.
[21] Jin X, Runt J. In preparation.
[22] Hayward D, Pethrick RA, Siriwittayakorn T. Macromolecules 1992; 25:1480.
[23] Russell TP, Ito H, Wignall GD. Macromolecules 1988;21:1703.
[24] Anastasiadis SH, Karatasos K, Vlachos G, Manias E, Giannelis EP. Phys Rev Lett 2000;84:915.
[25] Ngai KL. J Phys: Condens Matter 1999;11:A119.
[26] J Phys IV, Fr 2000;10:Pr7 [special issue].
[27] J Phys: Condens Matter 1999;11A [special issue].
[28] Park J-Y, McKenna GB. Phys Rev B 2000;61:6667.
[29] Kremer F, Huwe A, Arndt M, Behrens P, Schwieger W. J Phys: Condens Matter 1999;11:A175.
[30] Donth E. J Polym Sci, Polym Phys 1996;34:2881.
[31] Vaia RA, Sauer BB, Tse OK, Giannelis EP. J Polym Sci, Polym Phys 1997;35:59.
[32] Yamamoto K, Maruta A, Shimada S. Polym J 2001;3:584.
[33] Angell CA. J Non-Cryst Solids 1991;131–133:13.
[34] Gómez D, Alegría A, Arbe A, Colmenero J. Macromolecules 2001; 34:503.
[35] Zhang SH, Jin X, Painter PC, Runt J. Macromolecules 2002;35:3636.
[36] Sy JW, Mijovic J. Macromolecules 2000;33:933.
[37] Dionísio M, Fernandes AC, Mano JF, Correia NT, Sousa RC. Macromolecules 2000;33:1002.